

Phase-Changing Metamaterial Capable of Variable Stiffness and Shape Morphing

Ryan Poon and Jonathan B. Hopkins*

Herein, a metamaterial is introduced that achieves tunable stiffness properties according to uploaded instructions, which control the phase of low-melting-temperature metals embedded in elastomeric spherical shells at selected locations within the lattice's microarchitecture. A macroscale cubic lattice of gallium-filled silicone rubber spheres is fabricated as a proof of concept. Nickel-chromium (nickchrome) wires are threaded through the spheres within each row in the lattice so that current can be applied to specific rows to melt their gallium cores, thereby achieving a drop in the lattice's stiffness. Using this approach, the lattice can achieve a $3.7 \times$ increase in stiffness at 7% strain when the gallium cores are all solid compared with when they are all liquid. Larger increases in stiffness are possible for larger compression strains and with thinner silicone shells. Lattices with solid gallium cores experience buckling when compressed, but lattices with liquid gallium cores do not. Simulations demonstrate that cores can be liquified and resolidified much faster as they are scaled down in size, thus enabling rapid metamaterial stiffness control. Shape reconfiguration is also possible by liquifying select gallium cores at desired locations within the lattice, deforming it, and then resolidifying the cores to passively retain the lattice's shape.

Unlike traditional materials that achieve their properties from their composition, actively controlled metamaterials achieve their properties primarily from how their microarchitectures are structured and controlled via actuation. The ability to selectively control the stiffness and shape of individual elements within such microarchitectures has attracted significant attention for enabling a host of applications that would be difficult to achieve otherwise (e.g., an aircraft wing that changes its stiffness and shape at select locations in real time to eliminate vibrations, improve maneuverability, and decrease fuel consumption according to changing flight conditions).

A variety of approaches have been used to create metamaterial concepts that achieve such stiffness and/or shape tunability at desired locations using active control. Advanced approaches have utilized actuators, sensors, and microprocessors inserted inside constituent flexible cells that deform to achieve stiffness^[1] or shape changes^[2] using closed-loop control. Other approaches

R. Poon, Dr. J. B. Hopkins
Department of Mechanical and Aerospace Engineering
University of California, Los Angeles
Los Angeles, CA 90095, USA
E-mail: hopkins@seas.ucla.edu

The ORCID identification number(s) for the author(s) of this article can be found under <https://doi.org/10.1002/adem.201900802>.

DOI: 10.1002/adem.201900802

have utilized electromagnetic locks to alter the lattice stiffness by causing constituent beams to resist internal loads only when they are locked together rather than when they are disengaged.^[3] Other approaches have leveraged buckling elements that can be selectively actuated to achieve dramatic changes in system-level stiffness.^[4]

Although traditional phase-changing materials^[5] are most widely used in industry for a variety of applications (e.g., flexible electronics,^[6] stretchable sensing devices,^[7] and wearable electronic skin^[8]), some work has utilized them for achieving programmable stiffness as well. A tunable stiffness polydimethylsiloxane (PDMS) beam was built with microchannels filled with a low-melting-point alloy (LMPA) that froze at low temperatures to become stiffer but melted at high temperatures to become more flexible.^[9–11] Similar work used multilayer composite beams with plastic layers that could be heated to change the flexural stiffness of the beam.^[12] Others achieved

variable bulk compression moduli by heating polymer foam structures coated or infused with wax.^[13,14] Others have infused LMPA into a bicontinuous silicone foam,^[15] similarly attaining thermally controlled bulk reversible stiffness and shape memory. Despite their impressive functionality, none of these concepts achieve the ability to locally change stiffness and/or shape at select locations within a metamaterial lattice.

In this study, we propose a new kind of metamaterial that leverages the capabilities of LMPA phase-changing materials by organizing small spheres of such materials within periodic lattices of elastomeric shells embedded with electrical wiring that can change the phase of the LMPA on command via electrical heating. The concept is shown in Figure 1a. The metamaterial's periodic cells each consist of eight cubically packed gallium spheres within silicone rubber shells. In the center of these cells are integrated circuit (IC) chips that are externally powered with redundant power and ground lines shown as red and black, respectively, in Figure 1a. These IC chips can receive uploaded control commands that enable the gallium within any of their surrounding spheres to be melted by flowing current through nichrome wires (Figure 1a) that pass through the gallium and loop back to the IC chips. Such metamaterials could also be plumbed with tubes (not shown in the figure) that carry cooling fluid within the spheres to increase the speed so that their gallium cores can be solidified. In this way, 3D stiffness control could be achieved at select locations on demand within the

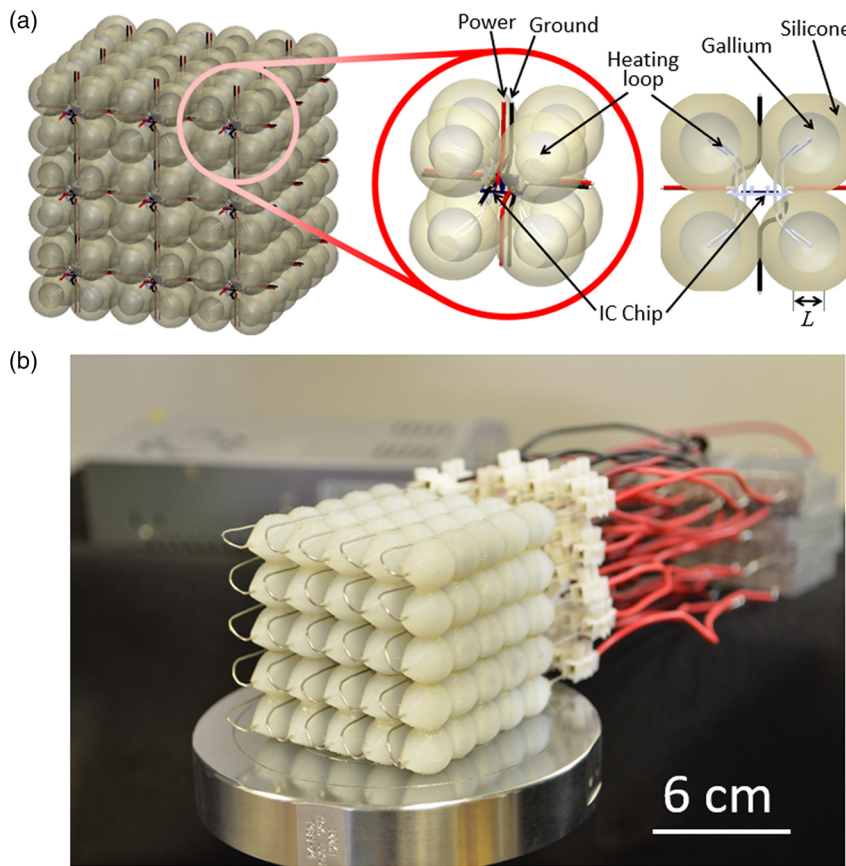


Figure 1. a) Concept design of an actively controlled phase-changing metamaterial with programmable stiffness and shape reconfigurability and b) a fabricated macroscale prototype $5 \times 5 \times 5$ lattice.

metamaterial. Moreover, different fractions of liquid and solid spheres could be evenly dispersed within a large lattice to achieve many different states of averaged stiffness between the two extreme stiffness states, where either all of the spheres are liquid or all of them are solid (i.e., analogue stiffness control is possible). Note that the design of Figure 1a could be cut in any way desired without altering its properties similar to natural materials. Although cutting the material in half, for example, may cause some cells on the lattice's cut surface to be permanently damaged or leak gallium, the lattice's wiring is sufficiently redundant and its interior cells are sufficiently self-contained to enable the metamaterial to continue to function without interruption as long as external power remains attached to at least one of its pairs of power and ground lines.

Such materials could also reconfigure their shape as desired if select gallium cores are melted, deformed, and then solidified in their deformed configuration. If the gallium cores within such deformed lattices are again liquified, they will passively return to their original shape. Simulations and experimental data collected from a simplified macroscale prototype (Figure 1b) of this idea demonstrate the concept's feasibility.

Five separate compression tests were conducted on the final lattice of Figure 1b for each of the lattice's two extreme phases (i.e., all of its gallium cores are solid or all of them are liquid). Videos of these tests are provided in the Supporting Information.

The effective stress, σ_{lattice} , imparted on the lattice was calculated by dividing the measured Instron force by $(nD)^2$, where n is the number of spheres in each side of the $n \times n \times n$ lattice (i.e., $n = 5$ for the lattice of Figure 1b) and D is the distance between the centers of each neighboring gallium sphere (i.e., $D = 16$ mm). The effective strain, $\epsilon_{\text{lattice}}$, imparted on the lattice was calculated by dividing the measured Instron displacement by nD .

The measured stress-strain plot of the lattice of Figure 1b with all-solid gallium cores is given in Figure 2a. Data were only collected up to 7% strain to conservatively prevent the solid gallium spheres from tearing out of their silicone shells. COMSOL was used to simulate the performance of the same lattice under the same loading conditions using the material properties and parameters detailed in Section 3 of Supporting Information. The simulated results are provided in Figure 2a up to 10% strain. A video of the simulation showing the lattice deforming up to 20% strain is provided in the Supporting Information. The simulation reveals that beyond 9% strain, the lattice buckles as the solid gallium spheres slide laterally inward as their silicone shells deform to accommodate the high compression strain.

The measured stress-strain plot of the lattice of Figure 1b with all-liquid gallium cores is shown in Figure 2b up to 10% strain. A video of the COMSOL simulation applied to this lattice, showing it deform up to 20% strain, is also provided in the Supporting Information. Note that no buckling occurs in the lattice when its

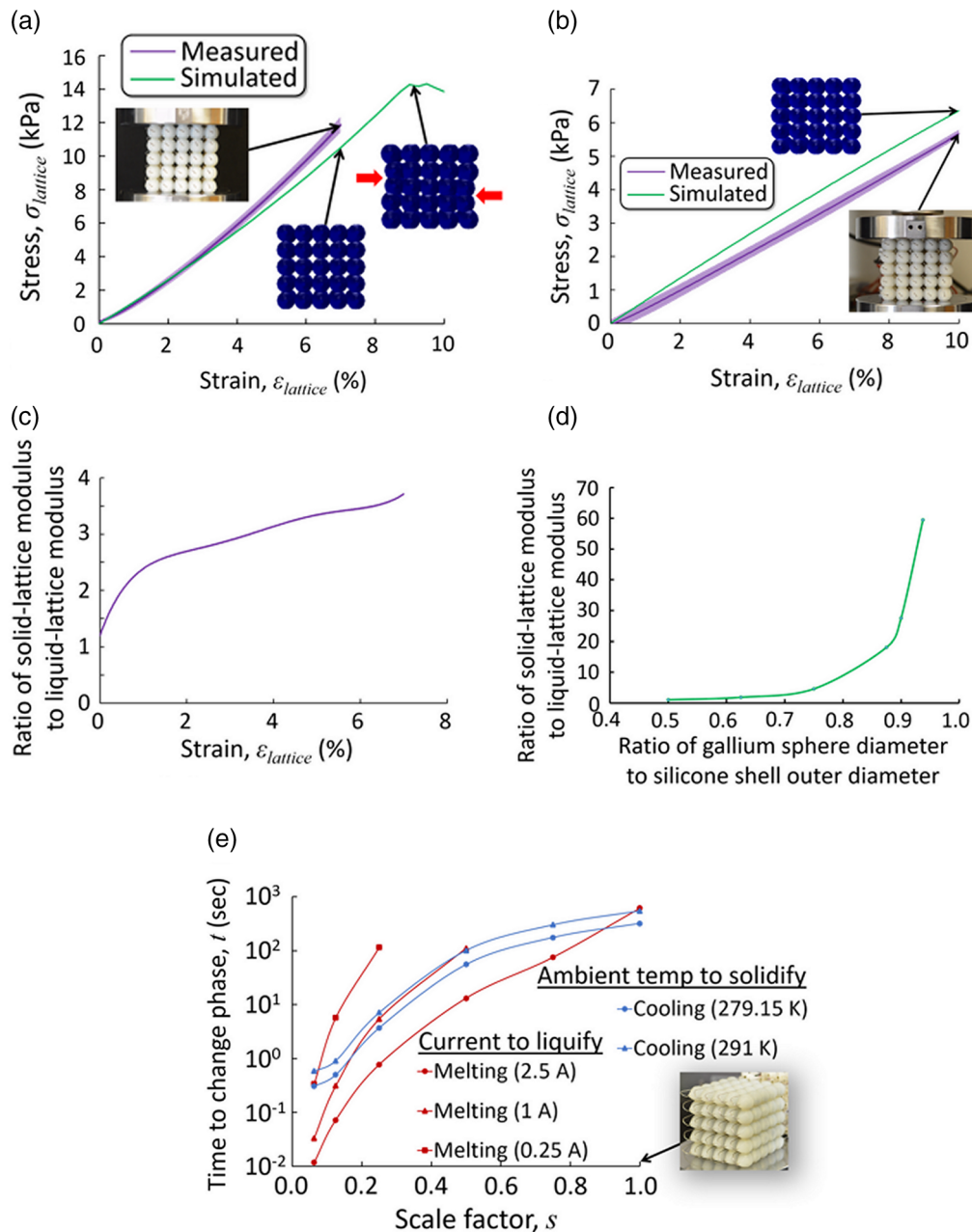


Figure 2. a) Experimental and simulation compression results for the lattice in Figure 1b with fully solid gallium spheres; b) experimental and simulation compression results for the same lattice with fully liquid gallium spheres; c) plot showing how many times stiffer the lattice in Figure 1b is when all of its gallium spheres are solid compared with when they are all liquid at different compression strains; d) plot showing how much stiffer lattices with fully solid gallium spheres are compared with when their gallium spheres are fully liquid as their gallium-sphere diameter to silicone-shell diameter ratio increases; and e) the time required to fully liquify and solidify gallium spheres encased within their elastomeric shells at different size scales and with different currents and ambient temperatures, respectively. The shaded error regions in (a) and (b) were generated using the results of five identical compression tests. The upper and lower bounds of these regions represent three standard deviations above and below the average values (shown as a dark purple line) calculated from these tests.

gallium cores are all liquid because the dominant mechanism that resists the compressive load of the Instron is the stretching of the silicone shells similar to water balloons being compressed.

Note that whereas the experimental results plotted in Figure 2a,b were produced by compressing a lattice with

nichrome wires that pass through the lattice's constituent gallium spheres, the simulations plotted in the same figures were generated without these nichrome wires. Further simulation studies, however, reveal that the nichrome wires have no appreciable effects on the simulated stress-strain plots of Figure 2a,b.

The plot of Figure 2c was generated by calculating the slopes of the measured data in Figure 2a for every strain up to 7% and dividing them by the slopes of the measured data in Figure 2b for corresponding strains. Thus, the plot of Figure 2c provides the ratio of the elastic modulus of the lattice of Figure 1b with all solid gallium cores to the elastic modulus of the same lattice with all liquid gallium cores for strains up to 7%. Note that the elastic modulus of the lattice with all solid cores is always larger than the elastic modulus of the lattice with all liquid cores. Moreover, note that the change in stiffness between these different phase lattices increases as they are strained in larger amounts. At 7% strain, the all-solid gallium lattice is $3.7 \times$ stiffer than the all-liquid gallium lattice, whereas when neither lattice is strained, the all-solid gallium lattice is only $1.3 \times$ stiffer than the all-liquid gallium lattice. These changes in stiffness can be increased further by increasing the ratio of the gallium-core diameter to the silicone-shell outer diameter (i.e., by decreasing the relative silicone shell thickness so that most of the lattice is gallium). Figure 2d shows this claim by using COMSOL to plot the ratios of the elastic moduli of lattices with all-solid gallium spheres to the elastic moduli of corresponding lattices with all-liquid gallium spheres versus the ratios of the lattices' gallium-sphere diameters to their silicone-shell outer diameters.

COMSOL was used to simulate how quickly the gallium spheres within the design of Figure 1b could fully liquify or solidify at different size scales for various currents and ambient temperatures, respectively (see Section 3 of Supporting Information for simulation details). Each of the three red plots in Figure 2e shows how the time that it takes the solid gallium spheres within the lattice of Figure 1b to fully liquify will vary as a function of different scale factors, s , when the spheres are melted using three different current values (i.e., 0.25, 1, and 2.5 A). Note that the smaller the sphere sizes are and the higher the current is that is used to melt them, the less time it takes to liquify the spheres and thus the faster the lattice could be controlled to reduce its stiffness. The two blue plots of Figure 2e show how the time that it takes melted gallium spheres within the lattice of Figure 1b to fully solidify will vary as a function of different scale factors, s , at two different ambient temperatures (i.e., 279.15 and 291 K). Note that the smaller the sphere sizes are and the lower the ambient temperature is, the less time it takes to solidify the spheres and thus the faster the lattice could be controlled to increase its stiffness. The plots of Figure 2e demonstrate that once the lattice of Figure 1b is scaled down so that its silicone spheres are small enough (i.e., <1 mm in size corresponding to a scale factor of $s < 0.06$) to classify their lattice as a metamaterial instead of a collection of macrosized spheres, the metamaterial could rapidly change its stiffness (i.e., the phase of its gallium cores) in <1 s.

Shape reconfiguration of the lattice of Figure 1b was also demonstrated by first melting the rows of spheres colored red in Figure 3a, by flowing current through those rows. When the gallium cores of those rows were fully liquified, metal slabs were placed at an angle on top of the lattice to deform it, as shown in the figure. While held in that deformed shape, all the gallium spheres were allowed to solidify at room temperature at which point the metal slabs were then removed. Figure 3b shows that the resulting lattice passively holds its deformed shape and will continue to do so until its gallium cores are again melted.

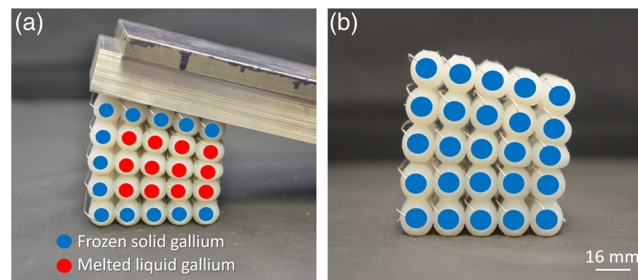


Figure 3. a) By liquifying select gallium cores within the lattice, the lattice can be deformed and held in place until all the gallium cores again solidify to achieve b) a metamaterial that can passively maintain its deformed shape. If the gallium cores are again liquified, the metamaterial will return to its original shape.

A metamaterial was introduced that consists of a lattice of elastomeric spheres filled with gallium cores that can be made to change their phase from solid to liquid and back at select locations within the lattice to control the material's overall stiffness and shape as desired. The thinner the elastomeric shells are and the more the lattice is compressed, the stiffer the all-solid gallium version of the lattice is compared with its all-liquid gallium version. Buckling instabilities can be eliminated by melting the gallium spheres within the lattice. We also demonstrated that as the elastomeric spheres are scaled down to their envisioned metamaterial size (i.e., <1 mm) they can be made to change phase rapidly enough to enable real-time stiffness control for enabling advanced applications. Such applications could include 1) endoscopic tools that are compliant as they maneuver through a body but then stiffen on command to enable the tool to cut or perform a procedure that requires rigidity; 2) materials that change their natural frequency on demand for eliminating or enhancing vibrations; and 3) armor that can actively change stiffness at select locations and thereby mitigate or redirect the flow of stress waves through their lattice caused by high speed impacts.

Experimental Section

Each row of the fabricated macroscale prototype (Figure 1b) was a necklace of 5 mm-diameter gallium spheres strung on a 26.6 cm-long nichrome cylindrical wire with a 0.032 in. diameter. The spheres were spaced 16 mm apart and each gallium sphere was embedded within a 16.76 mm-diameter Dragon Skin 10 Medium silicone rubber spherical shell. The diameter, labeled L in Figure 1a, of the circular region that joins each silicone shell together is 5 mm.

Two molding stages were required to fabricate the lattice in Figure 1b. The first molding stage enabled the gallium spheres to be strung onto each nichrome wire. Each half of the molds, which were 3D printed using a Stratasys uPrint SE Plus, possesses hemispherical cavities to form the gallium spheres and a groove to lay the nichrome wires through their centers (Figure 4a). Jet-Lube Rubber Lubricant was sprayed onto both halves of the mold to facilitate part release. A hand drill and clamps were used to shape the wires. The two mold halves were clamped together using screws (Figure 4b). The gallium was melted and then drawn into a syringe to be injected through the openings at the top half of the closed mold. A piece of frozen gallium was placed in contact with the liquid to seed the freezing process (Figure 4c). Once solidified, the "necklaces" of gallium beads were removed from the mold and were then suspended between the two halves of the second mold (Figure 4d). Both halves of this mold were also sprayed with lubricant and clamped together using

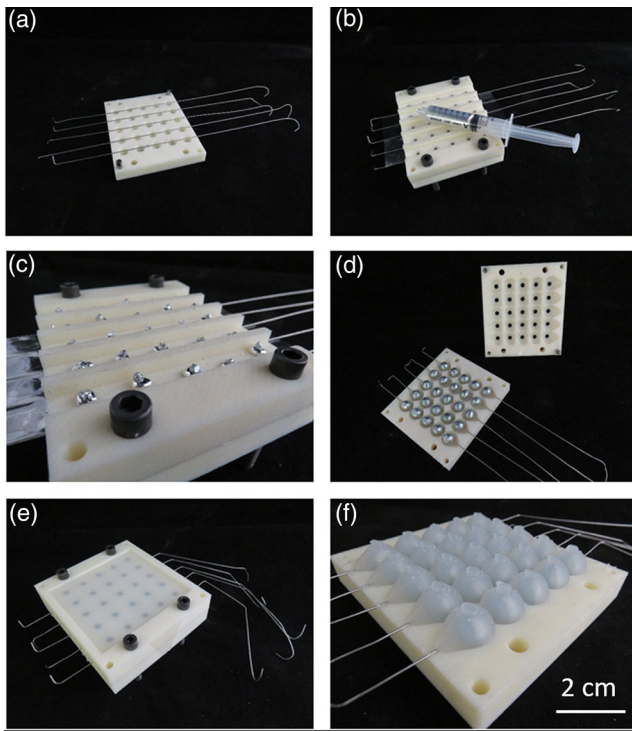


Figure 4. a) First mold with nichrome wires placed in grooves; b) other mold half clamped in place by screws so gallium could be injected into holes using a syringe to fill the mold; c) solid gallium chunks placed on holes to seed the solidification process; d) gallium-sphere “necklaces” placed in the second mold; e) silicone was injected and cured in the second mold once it was clamped together; and f) final layer removed from the second mold.

screws. 200 mL of Dragon Skin Part A and 200 mL of Part B were mixed and injected into the mold until the reservoir on the top half became full. The mold was placed into a vacuum chamber to remove air bubbles (Figure 4e). After curing, the lattice layer was removed, and the flash was clipped away (Figure 4f). Four more layers were created and epoxied together to form the $5 \times 5 \times 5$ lattice in Figure 1b. Additional fabrication details are provided in Section 1 of Supporting Information.

A JoyNano 5V 80A direct current power supply was used to heat up desired rows within the lattice of Figure 1b to selectively melt their gallium cores and thereby lower the lattice’s stiffness at targeted locations as desired. Each branch of the parallel circuit contained a 1.2Ω resistor (15 W power rating) in series with the nichrome wire, which had a resistance of 0.576Ω . Assuming ideal copper wires, the theoretical current and voltage drop across the nichrome wires were calculated to be 2.815 A and 1.622 V. To connect the copper wires to the nichrome wires, Rustark quick-connect screw clamping terminals were used due to the incompatibility between nichrome and solder. An Instron testing machine (Model 5966) was used to measure the mechanical properties of the lattice of Figure 1b for different phases of its gallium cores. Additional details about the electronics and experimental test setup are provided in Section 2 of Supporting Information.

Supporting Information

Supporting Information is available from the Wiley Online Library or from the author.

Acknowledgements

This work was supported by AFOSR award number FA9550-18-1-0459. The authors acknowledge program officer Byung “Les” Lee.

Conflict of Interest

The authors declare no conflict of interest.

Keywords

low-melting-point metals, phase-changing materials, programmable meta-materials, shape-reconfigurable architected materials, variable stiffness

Received: July 2, 2019

Revised: September 1, 2019

Published online:

- [1] Y. Song, P. C. Dohm, B. Haghpanah, A. Vaziri, J. B. Hopkins, *Adv. Eng. Mater.* **2016**, *18*, 1113.
- [2] L.A. Shaw, J.B. Hopkins, *J. Mech. Robot.* **2015**, *8*(2): 021019
- [3] B. Haghpanah, H. Ebrahimi, D. Mousanezhad, J. B. Hopkins, *Adv. Eng. Mater.* **2016**, *18*, 643.
- [4] C. B. Churchill, D. W. Shahan, S. P. Smith, A. C. Keefe, G. P. McKnight, *Sci. Adv.* **2016**, *2*, e1500778.
- [5] N. Kazem, T. Hellebrekers, C. Majidi, *Adv. Mater.* **2017**, *29*, 1605985.
- [6] A. C. Siegel, D. A. Bruzewicz, D. B. Weibel, G. M. Whitesides, *Adv. Mater.* **2007**, *19*, 727.
- [7] Y. L. Park, B. R. Chen, R. J. Wood, *IEEE Sens. J.* **2012**, *12*, 2711.
- [8] J. W. Boley, E. L. White, G. T. C. Chiu, R. K. Kramer, *Adv. Funct. Mater.* **2014**, *24*, 3501.
- [9] B. E. Schubert, D. Floreano, *Rsc. Adv.* **2013**, *3*, 24671.
- [10] P. S. Owuor, S. Hiremath, A. C. Chipara, R. Vajtai, J. Lou, D. R. Mahapatra, P. M. Ajayan, *Adv. Mater. Interfaces*. **2017**, *4*, 1700240.
- [11] E. A. Allen, L. D. Taylor, J. P. Swensen, *Smart Mater. Struct.* **2019**, *4*, 074007.
- [12] F. Gandhi, S.-G. Kang, *Smart Mater. Struct.* **2007**, *16*, 1179.
- [13] N. G. Cheng, A. Gopinath, L. Wang, K. Iagnemma, A. E. Hosoi, *Macromol. Mater. Eng.* **2014**, *299*, 1279.
- [14] A. Balasubramanian, M. Standish, C. J. Bettinger, *Adv. Funct. Mater.* **2014**, *24*, 4860.
- [15] I. M. Van Meerbeek, B. C. Mac Murray, J. W. Kim, S. S. Robinson, P. X. Zou, M. N. Silberstein, R. F. Shepherd, *Adv. Mater.* **2016**, *28*, 2801.